INTERNATIONAL
Agrophysics
www.international-agrophysics.org

Int. Agrophys., 2023, 37, 1-14
doi: 10.31545/intagr/156027

Application of land use modes in the spatial prediction of soil organic carbon in urban green spaces**

Xiaoxue Guo[1], *Zhijun Liu*[2], *Dongli Gao*[3,1], *Chengli Xu*[2], *Kexin Zhang*[1], *and Xianzhao Liu*[1]*

[1]Key Laboratory of Forest Management and Growth Modelling, National State Forestry and Grassland Administration, Research Institute of Forest Resource Information Techniques, Chinese Academy of Forestry, Beijing 100091, China
[2]Ecological Construction Investment Company Limited, Xiong'an Group, Xiong'an 071699, China
[3]Industry Development and Planning Institute, NFGA, Beijing 100010, China

Received August 30, 2022; accepted October 24, 2022

Abstract. The challenge of predicting soil organic carbon distribution accurately has received great attention in order to support urban green space soil management during climate change. This study compared four geostatistical methods: kriging combined with land use, ordinary kriging, inverse distance weighting and radial basis function, to predict the spatial distribution patterns of soil organic carbon content and soil organic carbon density in the Xiong'an New Area, estimate organic carbon stocks, and assess the role of land use types in the spatial prediction of soil organic carbon stocks. The results showed that the soil organic carbon content decreased with increasing soil depth, and was significantly affected by different land use types ($p<0.05$). The correlation coefficient values of kriging combined with land use were on average 0.229 higher than those of other methods. The root mean squared error and the mean absolute error of kriging combined with land use were on average 0.148 and 0.139 lower than those of the other methods. Kriging combined with land use has a greater advantage over other methods in predicting the spatial distribution of soil organic carbon content, and also the spatial distribution of soil organic carbon density and the spatial distribution of soil organic carbon, the prediction results of the four interpolation methods were similar. The average soil organic carbon density was 2085 Gg (0-30 cm) and 1363 Gg (30-60 cm). In conclusion, land use type clearly influences the spatial distribution of soil organic carbon in urban areas, and by using land use type as auxiliary data, we can obtain a more accurate spatial distribution of soil organic carbon and predict the total storage capacity of the soil. This study may result in significant advances in the spatial prediction of soil organic carbon for urban areas.

*Corresponding authors e-mail: lxz9179@163.com
**This work was supported by the Chinese Academy of Forestry (CAFYBB2019ZB005; 2019-2022).

Keywords: geostatistics, soil organic carbon, spatial distribution, urban land use, Xiong'an New Area

INTRODUCTION

Soil is the most crucial and also the largest carbon reservoir in terrestrial ecosystems (Yang *et al*., 2007), it stores more than three-quarters of the world's terrestrial carbon and plays a vital role in the terrestrial carbon cycle (Johnston *et al*., 2004; Lal, 2004). As an essential component of the soil (Scharlemann *et al*., 2014), soil organic carbon (SOC) is a major participant in the soil-atmosphere carbon cycle, with litter originating from vegetation falling continuously and storing carbon in the the form of SOC through assimilation, SOC also emits CO_2 to the atmosphere through decomposition (Kirschbaum, 2000; Janzen, 2004; Keith *et al*., 2021). Soil carbon sequestration can effectively mitigate the greenhouse effect and also reduce the heat island effect to some extent, it is regarded as one of the keys to solving the problem of climate change (Viscarra *et al*., 2014; Minasny *et al*., 2017; Blais, 2021). SOC is also a basic indicator of soil fertility, and the level of SOC directly affects the potential productivity of vegetation and the general quality of the environment, it plays a vital role in maintaining the sustainability of the ecosystem (Stockmann *et al*., 2013; Liu *et al*., 2017).

SOC content depends on both the intrinsic and extrinsic soil factors. In general, natural factors (*e.g.* climate, vegetation, and topography) and the heterogeneity of human activities (*e.g.* fossil fuel burning, land use change, and fertilizer application) are the main causes of dynamic changes in SOC at different spatial scales (Gelaw *et al*., 2014). Since the Industrial Revolution, the impact of human activity has led to accelerated global warming (Panja, 2021). Rising temperatures will in turn accelerate carbon emissions from the soil into the atmosphere and thus the accumulation of CO_2 (Davidson and Janssens, 2006; Hopple *et al*., 2020). The soil carbon sequestration capacity and its duration will also be reduced, resulting in a decrease in SOC content and hence a decline in soil quality and in the productivity of biomass (Lal, 2004; Luo, 2020). In particular, with the continuous increase in the level of social development, the degree of damage to the original ecosystem caused by human activities has intensified, resulting in significant differences in the distribution of SOC at different spatial scales. This phenomenon not only affects regional land use planning but also poses a more serious challenge to environmental management (Mabit and Bernard, 2010; Vasenev *et al*., 2014; Xu *et al*., 2016). Therefore, accurate predictions of soil organic carbon and its spatial distribution pattern are of great significance in managing and utilizing land resources in response to climate change.

In recent years, with the continuous development of geostatistics and GIS technology, the method of combining both technologies has been widely used to evaluate the spatial distribution of various soil attributes and to explore the influence of different factors on the spatial distribution of soil attributes (Yao *et al*., 2006; Minasny *et al*., 2017). There have been many studies concerning the spatial distribution of SOC and the factors affecting spatial distribution, including natural factors such as soil depth, topographic elements, and elevation (Zhang *et al*., 2018; Li *et al*., 2019), anthropogenic factors such as deep soil flipping have also been studied (Schiedung *et al*., 2019). These studies were focused on a certain land use mode (*e.g.* farmland) or various land use types with less human disturbance, and rarely involved urban areas where humans gather in large numbers. At present, the ecological crisis has become a growing concern for countries worldwide. In response to the dual challenges of global climate change and accelerated urbanization, the promotion of eco-city construction has gradually become an international policy priority (Joss *et al*., 2013). "Carbon" has been placed at the centre of eco-city policy and construction. In this context, changes in SOC content and spatial distribution have not only had a significant impact on the global carbon cycle and greenhouse gas emissions, but are also particularly important for the construction of the optimal eco-city (Deng *et al*., 2018; Ye *et al*., 2021). At the same time, the differences between different land use types in urban areas have become more and more significant after long-term human development and transformation. This phenomenon leads to an effective increase or decrease in SOC content in different areas, which greatly impacts the spatial distribution of SOC (Boubehziz *et al*., 2020; Barreto *et al*., 2021). Therefore, exploring the influence of land use types on the spatial distribution of SOC, and determining the of SOC stock (*SOCS*), forms an important foundation for eco-city construction based on original urban planning, especially for greening construction, environmental protection, and the rational development of land resources (Yan *et al*., 2015).

The Xiong'an New Area is a state-level new area established in China in 2017 as part of an effort to centralize the process of transferring non-capital functions from Beijing to other cities (Zou and Zhao, 2018). The eco-city is one of the priorities of the planned development of the Xiongan New Area. This study is based on field survey data from the east of Xiong'an New Area, and uses kriging combined with land use (KLU) and three other traditional interpolation methods; inverse distance weighting (IDW), radial basis function (RBF), and ordinary kriging (OK), to (1) study the spatial variability in SOC at two depths (0-30, 30-60 cm) and analyse the effect of land use on SOC, (2) analyse the spatial distribution pattern of SOC content by combining four interpolation methods, (3) analyse the spatial distribution pattern of SOC density (*SOCD*) by combining different calculation and interpolation methods, (4) calculate the regional *SOCS* based on the interpolation results. This study may serve to provide a theoretical basis to illustrate the spatial distribution characteristics of SOC in the urbanization process, to show the extent to which land resources are used in a reasonable way, and may optimize the process of conducting urban planning and land management in the future.

MATERIALS AND METHODS

The study area (Fig. 1) is located in the east of the Xiong'an New Area (115°59'-116°19' E, 38°46'-39°10' N), Hebei Province, China, it is at the core of the construction of an ecological transition zone of the Beijing-Tianjin-Baoding Plain, which covers a total area of 677.6 km². The terrain is flat and open, and dominated by low-altitude plains. The primary soil type is alluvial soil, and the soil texture is mainly light flux loam. The weather is typical of a warm temperate semi-arid and semi-humid monsoon climate, with four distinct seasons of rain and heat, with an average annual temperature of 12.9°C and average annual precipitation of about 566.1 mm, mainly concentrated in the July and August period (Hebei Statistical Bureau, 2021).

In this study, a systematic sampling approach was adopted, using the CreateFishnet function in the ArcGIS software to generate soil sampling sites with a grid spacing of 2.5×2.5 km, a total of 91 soil survey points were selected, sampling points which included water bodies,

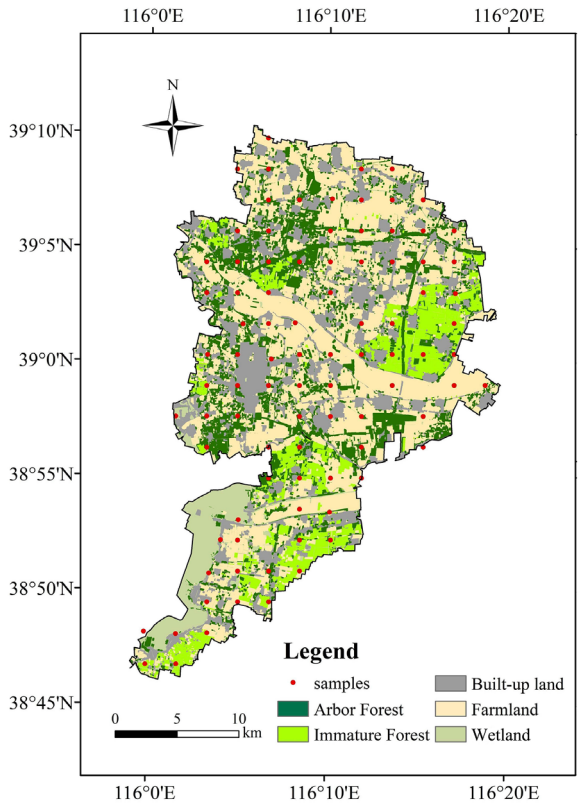

Fig. 1. Location map of the study area and distribution of the sampling sites.

buildings, and hardened roads were excluded. The soil survey was carried out using GPS navigation to the sampling points from late October to mid-November in 2020.

A five-point sampling method was used to collect soil samples from the upper layer (0-30 cm) and lower layer (30-60 cm) of the soil at the sampling point and also from four nearby corners, with a soil weight of not less than 300 g being collected at each point. The upper and lower layers of soil from different points were mixed using equal masses and returned to the laboratory. Then they were successively air-dried, ground, and sieved before being placed under observation for relevant indicators. The potassium dichromate-external heating method was used to determine the SOC content, and the drying method determined the soil bulk density (SBD) (Bao, 2005).

The semivariance function is a unique analytical tool in geostatistics and is widely used to describe the variability in the spatial structure of soil properties (Blanchet *et al*., 2017). If a soil property has second-order stationarity, its semivariance function $\gamma(h)$ is calculated as follows:

$$\gamma(h) = \frac{1}{2N(h)} \sum_{i=1}^{N(h)} [Z(x_i) - Z(x_i + h)]^2 \ , \qquad (1)$$

where: $N(h)$ is the number of point pairs spaced at h, and $Z(x_i)$ and $Z(x_i+h)$ are the values at points x_i and x_i+h respectively.

The semivariance function has several parameters, sill ($C_0 + C$), nugget (C_0) and range. The ratio of the nugget to the sill ($C_0/(C_0 + C)$) reflects the spatial correlation of the original data. The lower the ratio, the closer the spatial correlation (Cambardella *et al*., 1994). Common models which fit the semivariance function include exponential, Gaussian, spherical, *etc.* The optimal semivariance model was selected based on the determination coefficient (R^2) being as close as posiblepossible to 1 and residuals (RSS) being as low as possible.

OK is the most basic kriging method. It uses a semivariance function to calculate the mean degree of difference between the unsampled point and the neighbouring sampling points (Robinson and Metternicht, 2006):

$$\hat{Z}(x_0) = \sum_{i=1}^{n} \lambda_i z(x_i) \ , \qquad (2)$$

where: $\hat{Z}(x_0)$ is the predicted value at the unsampled point x_0, $z(x_i)$ is the observed value at the sampling point x_i, n is the number of samples, and λ_i is the weight which depends not only on the distance between the unsampled point and the sampling point, but also on the overall spatial layout based on the sampling point.

IDW is one of the most commonly applied deterministic interpolation methods for spatial interpolation in soil science. It is assumed that the value of the unsampled point is the weighted average of the sampling points in the neighbourhood around the unsampled point (Robinson and Metternicht, 2006). The weight assigned to the unsampled point is equivalent to the inverse of its distance from the sampling point (Bhunia *et al*., 2016):

$$\hat{Z}(x_0) = \frac{\sum_{i=1}^{n} z(x_i) d_i^{-p}}{\sum_{i=1}^{n} d_i^{-p}} , \qquad (3)$$

where: $\hat{Z}(x_0)$ is the predicted value at the unsampled point x_0, $z(x_i)$ is the observed value at the sampling point, d_i is the distance between the unsampled point and the i-th sampling point, and p is the weight.

RBF predicts the unsampled points by generating a smooth surface from all known sampling points.

KLU is an extension of the kriging method. Natural factors do not influence the spatial distribution of SOC content to a significant extent because the study area is flat and has a single soil type without significant heterogeneity. Land use type, which is the most apparent heterogeneity due to human activities in the study area, was used as an auxiliary variable in order to reduce the uncertainty it added to the overall prediction of the study area.

Based on the current status of land use in the 2018 and 2020 field surveys and the needs of the study, the land use types in the study area were classified into five categories: built-up land, arbour forest (existing farmland shelterbelt

and nontimber product forest in the Xiong'an New Area), immature forest (new plantations planted after the establishment of Xiong'an New Area and nursery), wetland and farmland (Fig. 1), of which the built-up land included bare land and barren hills (Ministry of Natural Resources, People's Republic of China, 2017). Based on the specific location of the sampling sites in Fig. 1 and the field survey results, the land use types of the sampling sites were judged. The sample points of the built-up land, arbour forest, immature forest, wetland and farmland were 19, 13, 15, 5 and 39, respectively. The observed value of each sampling point $Z(x_{ki})$ was divided into the sum of the mean value of the same land use type $\mu(t_k)$ and the residual $r(x_{ki})$. The formula was expressed as follows:

$$Z(x_{ki}) = \mu(t_k) + r(x_{ki}) \ , \tag{4}$$

where: x_{ki} is the location of the sample point $Z(x_{ki})$ and t_k is the land use type to which the sample point belongs.

The residuals $r(x_{ki})$ were kriged as a new regional variable and the predicted value of each unsampled point $\hat{Z}(x_{ki})$ was the sum of the mean land use type $\mu(t_k)$ and the predicted value of the residuals $\hat{r}(x_{kj})$:

$$\hat{Z}(x_{kj}) = \mu(t_k) + \hat{r}(x_{kj}) \ . \tag{5}$$

Two methods were used to calculate the *SOCD* in this study, then the *SOCS* of each method was calculated:

1. The SOC and SBD of each sampling point were used to calculate the *SOCD* of the sampling point. Then the obtained *SOCD* of the sampling point was used for spatial analysis in order to predict the spatial distribution of *SOCD* in the study area. Finally, the *SOCS* of the study area was predicted.

2. A spatial analysis was performed on the actual SOC and SBD data of the sampling points separately, and the *SOCD* of the whole study area was calculated using a raster calculation. Thus, the spatial distribution of *SOCD* was predicted, and the *SOCS* of the study area was calculated.

The *SOCD* values were calculated at various soil depths using the following equation:

$$SOCD_r = \frac{B_r C_r H_r}{100} \ , \tag{6}$$

where: $SOCD_r$ is the *SOCD* in layer r (kg m^{-2}), B_r is the SBD in layer r (g cm^{-3}), C_r is the SOC content in layer r (g kg^{-1}) and H_r is the thickness of the soil layer in layer r.

A spatial interpolation was performed using four interpolation methods in order to generate *SOCS* surfaces for the entire study area, which were then exported as raster layers with a resolution of 100×100 m. *SOCS* (Gg) was then calculated using the following equation:

$$SOCS = \sum_{i}^{n} (socd_i \ S \ 10^{-6}) \ , \tag{7}$$

where: $socd_i$ is the density of each grid (kg m^{-2}), and S is the area of each grid (m^2).

The *SOCD* values obtained using Method 1 are written as $SOCD^1$, and the overall *SOCS* are written as $SOCS^1$. The *SOCD* in Method 2 are written as $SOCD^2$, and the overall *SOCS* are written as $SOCS^2$.

The cross-validation method was used to test the prediction accuracy of different interpolation methods in the study area. The evaluation indicators included the root mean squared error (*RMSE*), the mean absolute error (*MAE*), and the Pearson correlation coefficient R. Larger R values, and lower *RMSE* and *MAE* values indicate a higher prediction accuracy.

$$RMSE = \sqrt{\frac{1}{n}\sum_{i=1}^{n}(x_i - x_j)^2} \ , \tag{8}$$

$$MAE = \frac{1}{n}\sum_{i=1}^{n}|(x_j - x_i)| \ , \tag{9}$$

$$\mathrm{R} = \frac{\sum_{i=1}^{n}\left(x_i - \bar{x}_i\right)\left(x_j - \bar{x}_j\right)}{\sqrt{\sum_{i=1}^{n}\left(x_i - \bar{x}_i\right)^2}\sqrt{\sum_{i=1}^{n}\left(x_j - \bar{x}_j\right)^2}} \ , \tag{10}$$

where: n is the number of validation points, x_i is the observed value of the sampling points and x_j is the predicted value of the sampling points.

RESULTS

The descriptive statistics of SOC content, SBD, and $SOCD^1$ in the study area are shown in Table 1. The SOC content ranged from 1.96~13.25 g kg^{-1}, SBD ranged from 0.95~1.69 g cm^{-3} and $SOCD^1$ ranged from 0.87~5.68 kg m^{-2}. As the soil layer depth increased, the mean of the SOC content decreased by 35.96%, the mean of $SOCD^1$ decreased by 33.66%, and the mean of SBD increased by 4.32%. The coefficient of variation (CV) reflects the degree of overall variability in the sample point values (Tang *et al*., 2017). The spatial variability of SBD was found to be weak. The CV values of SOC content and $SOCD^1$ varied from 35.95 to 44.85, which indicated a moderate degree of variability.

The analysis of variance (ANOVA) results showed that the SOC content and $SOCD^1$ were significantly different between the different land use types ($p<0.05$), while the differences in SBD were not significant. Fig. 2 shows the mean variation in SOC content and $SOCD^1$ between different land use types. In the upper soil layer (0-30 cm), built-up land was found to have the lowest mean SOC content (5.42 g kg^{-1}) and mean *SOCD* (2.17 kg m^{-2}), about 70% of the average SOC content and 71% of the average $SOCD^1$, respectively; immature forest had the highest mean SOC content (9.26 g kg^{-1}), about 1.71 times that of built-up land; arbour forest had the highest mean $SOCD^1$ (3.49 kg m^{-2}), about 1.61 times that of built-up land;

Table 1. Descriptive statistics of SOC content, SBD and *SOCD*[1]

Soil properties	Soil depth (cm)	Sample	Max	Min	Mean	SD	CV (%)	Skewness	Kurtosis
SOC (g kg^{-1})	0-30	91	13.25	2.31	7.73	2.80	36.22	0.14	–0.84
	30-60	91	12.84	1.96	4.95	2.22	44.85	1.06	1.07
SBD (g cm^{-3})	0-30	91	1.69	0.99	1.33	0.15	11.28	0.05	–0.18
	30-60	91	1.67	0.95	1.39	0.13	9.35	–0.67	1.09
SOCD[1] (kg m^{-2})	0-30	91	5.68	1.04	3.06	1.10	35.95	0.26	–0.52
	30-60	91	3.94	0.87	2.03	0.79	38.92	0.54	–0.71

SOC – soil organic carbon content, SBD – soil bulk density, *SOCD*[1] – soil organic carbon density for each sample point obtained using Method 1, Max – maximum value, Min – minimum value, Mean – mean value, SD – standard deviation, CV – coefficient of variation.

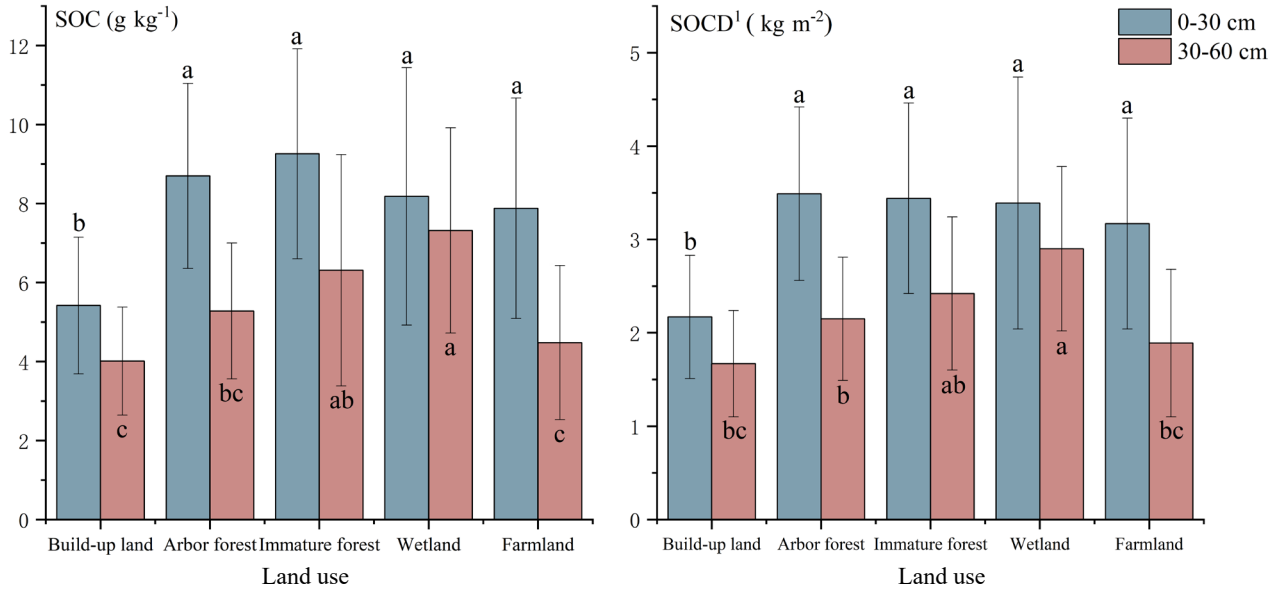

Fig. 2. SOC content and *SOCD*[1] for different soil layers and different land use types. Different lower case letters indicate a significant difference among the different land use types concerning the same soil properties for that layer at 0.05 significance level. The error bars denote the standard error of the mean.

the SOC content and *SOCD*[1] of the remaining land use types did not differ significantly. In the lower soil layer (30-60 cm), the mean SOC content (4.01 g kg^{-1}) and mean *SOCD*[1] (1.67 kg m^{-2}) were equally lowest in built-up land; the wetlands had the wwhighest mean SOC content (7.32 g kg^{-1}) and *SOCD*[1] (2.90 kg m^{-2}), which were about 1.83 and 1.74 times higher than the values found for the built-up land, respectively.

The Kolmogorov-Smirnov (K-S) test was used to test the normality of the original values and their residuals of SOC content, SBD, and *SOCD*[1]. After the natural logarithmic transformation of the skewed values, all data are normally distributed and may be analysed geometrically.

The optimal semivariance function fitting model was selected based on the R^2 value closest to 1 and the smallest RSS value, the specific model parameters are shown in Table 2. In the upper soil layer, the original values for SBD showed a pure nugget effect, and the optimal semivariance function model for the residual values was a Gaussian model. The optimal semivariance model for SOC content and *SOCD*[1] were spherical, and the residual values were exponential. In the lower soil layer, the optimal semivariance model for the original values of the SOC content and *SOCD*[1] were spherical, while for all of the other optimal semivariance models they were Gaussian. Some differences were found between the model parameters of the different approaches (Fig. 3). The $C_0/(C_0+C)$ values of the original values were between 0.62 and 1.00, they all had weak spatial correlations. The $C_0/(C_0+C)$ values of the residual data for both SOC content and *SOCD* decreased to different degrees compared to the original data. Meanwhile, the C_0 and C_0+C values of the residual data were lower than those of the original data with the exception of the log-transformed values.

The correlation between the observed and the predicted values of SOC content, *SOCD*[1] and *SOCD*[2] for the four interpolation methods are shown in Fig. 4. The accuracy and stability of the four interpolation methods were also assessed using *RMSE*, *MAE* and R (Table 3). The results showed that KLU had a significant advantage over the other

Table 2. Best-fit semivariance models and their parameters for the various prediction approaches

Soil depth (cm)	Soil properties	Approaches	Distribution	Models	C_0	C_0+C	$C_0/(C_0+C)$	Range (km)	R^2	RSS
0-30	SOC	OK	Normal	Spherical	6.499	8.296	0.78	14.57	0.94	0.13
		KLU	Normal	Exponential	3.370	6.741	0.50	12.33	0.96	0.12
	SBD	OK	Normal	Pure nugget effect	0.021	0.021	1.00	–	–	6.92×10^{-6}
		KLU	Normal	Gaussian	0.019	0.020	0.93	28.66	0.45	5.05×10^{-6}
	SOCD[1]	OK	Normal	Spherical	1.008	1.261	0.80	17.86	0.98	2.31×10^{-3}
		KLU	Normal	Exponential	0.120	1.015	0.12	6.54	0.93	5.76×10^{-3}
30-60	SOC	OK	Lognormal	Spherical	0.132	0.212	0.62	19.57	0.88	5.79×10^{-4}
		KLU	Normal	Gaussian	3.041	5.484	0.55	27.97	0.96	0.144
	SBD	OK	Normal	Gaussian	0.014	0.019	0.72	20.69	0.88	3.60×10^{-6}
		KLU	Normal	Gaussian	0.013	0.016	0.75	18.43	0.82	4.34×10^{-6}
	SOCD[1]	OK	Lognormal	Spherical	0.134	0.167	0.80	17.91	0.76	3.51×10^{-4}
		KLU	Normal	Gaussian	0.455	0.574	0.79	16.95	0.65	5.64×10^{-3}

OK – original values, KLU – residual values. Other explanation as in Table 1.

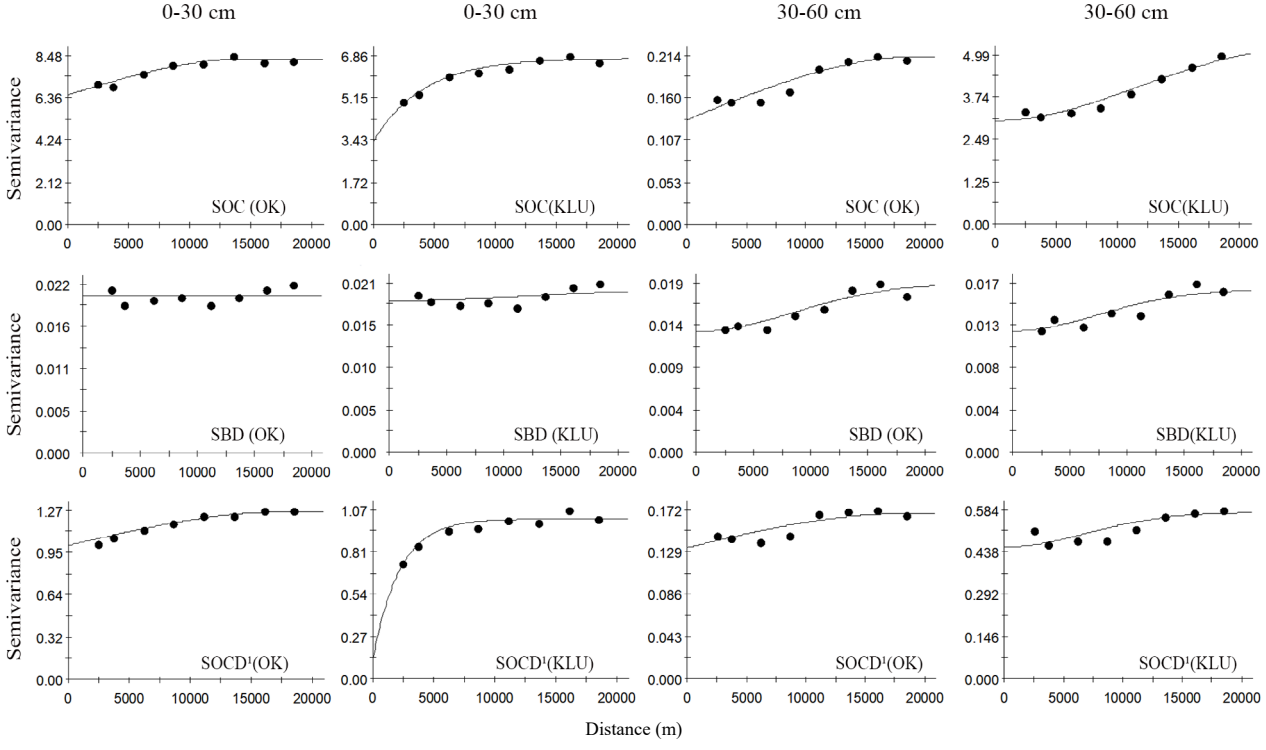

Fig. 3. Semivariograms of original values (OK) and their residuals (KLU) for SOC, SBD and *SOCD*[1].

three interpolation methods. The correlations between the predicted values and the observed values obtained using KLU all reached a significant level ($p<0.01$). In the upper soil layer, the R values of KLU for SOC content, *SOCD*[1] and *SOCD*[2] were 0.476, 0.389 and 0.425, respectively, which were on average 0.326, 0.280, 0.323 higher than those of the other three methods. The *RMSE* values of KLU for SOC (2.459), *SOCD*[1] (1.028) and *SOCD*[2] (0.999) were all the lowest values, and had averages of 0.376, 0.101 and 0.132 less than those of the other three methods. The *MAE* of KLU was also found to be closest to 0. In the lower soil layer, compared to the other interpolation methods, KLU on average increased in terms of R values by 0.112 (SOC), 0.177 (*SOCD*[1]) and 0.156 (*SOCD*[2]), with an average decrease in *RMSE* compared to the other interpolation methods of 0.153 (SOC), 0.068 (*SOCD*[1]) and 0.061 (*SOCD*[2]). The *MAE* of KLU was also found to be closest to 0.

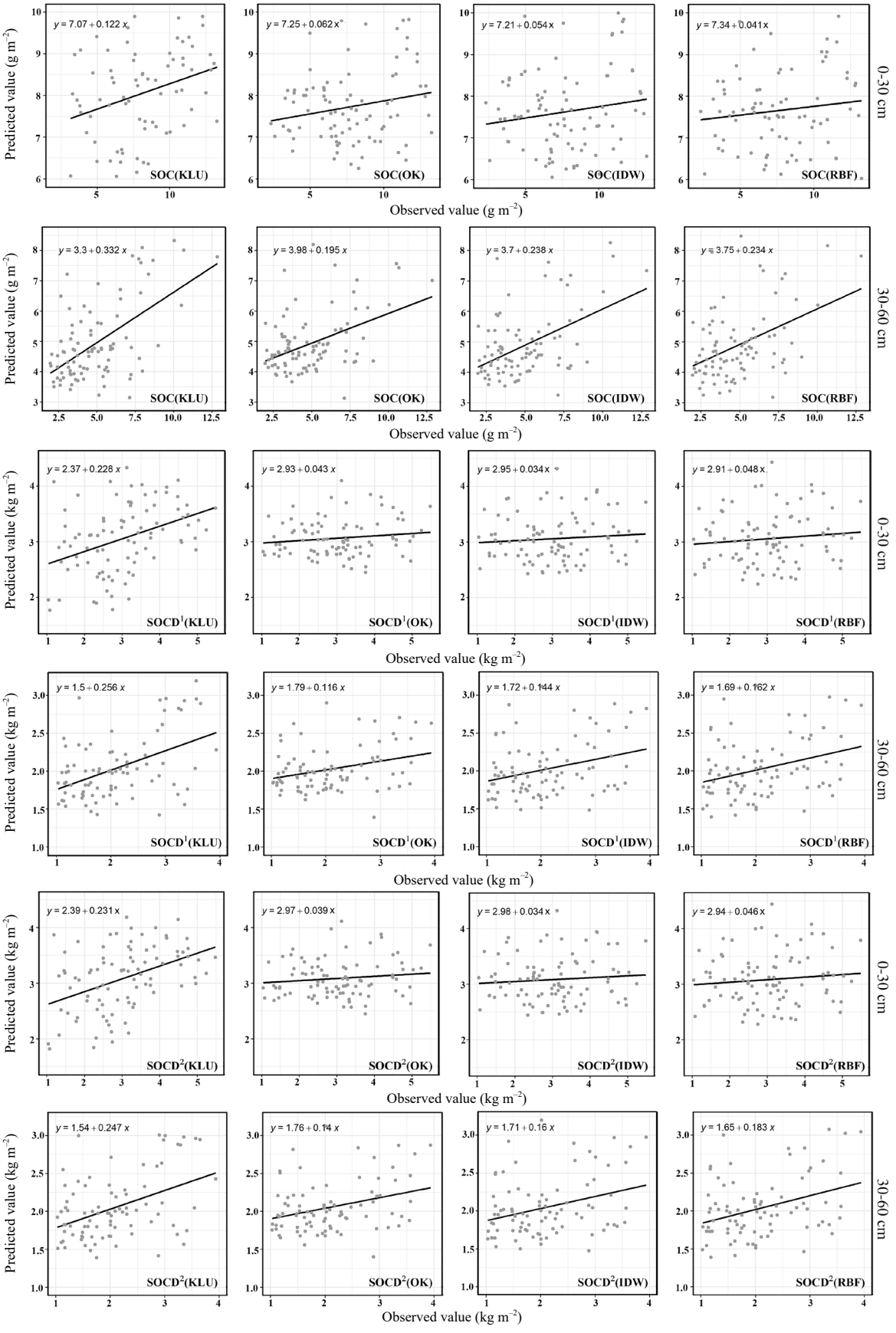

Fig. 4. Scatter plots of predicted and observed values for SOC, *SOCD*[1] and *SOCD*[2].

Table 3. Precision evaluation indices of different interpolation methods

Soil depth (cm)	Soil properties	Approaches	*RMSE*	*MAE*	R
0-30	SOC	KLU	2.459	2.068	0.476**
		OK	2.789	2.329	0.163
		IDW	2.847	2.355	0.138
		RBF	2.868	2.399	0.149
	SOCD[1]	KLU	1.028	0.836	0.389**
		OK	1.103	0.908	0.135
		IDW	1.139	0.920	0.083
		RBF	1.144	0.917	0.109
	SOCD[2]	KLU	0.999	0.811	0.425**
		OK	1.108	0.917	0.122
		IDW	1.139	0.919	0.081
		RBF	1.146	0.917	0.103
30-60	SOC	KLU	1.810	1.393	0.573**
		OK	1.981	1.615	0.442**
		IDW	1.963	1.589	0.462**
		RBF	1.943	1.567	0.480**
	SOCD[1]	KLU	0.670	0.537	0.486**
		OK	0.755	0.624	0.297**
		IDW	0.761	0.618	0.307**
		RBF	0.758	0.611	0.323**
	SOCD[2]	KLU	0.694	0.535	0.482**
		OK	0.755	0.624	0.313**
		IDW	0.758	0.612	0.323**
		RBF	0.755	0.605	0.341**

**Iindicates an extremely significant correlation at the 0.01 level. Other explanation as in Table 1.

In comparing the two methods of predicting *SOCD*, the KLU prediction accuracy of *SOCD*[2] was found to be highest in the upper soil layer (*RMSE*=0.999, *MAE*=0.811, R=0.425); the KLU prediction accuracy of *SOCD*[1] was found to be highest in the lower soil layer (*RMSE* = 0.690, *MAE* = 0.537, R = 0.486).

The SOC content and *SOCD* spatial distribution maps generated using KLU, OK, IDW and RBF are presented in Fig. 5 and Fig. 6. The high and low distribution of the SOC content and *SOCD* may be clearly determined from the colour changes in the interpolation maps. In terms of overall distribution, the distribution maps of *SOCD*[1] and *SOCD*[2] were highly consistent with the predicted SOC content distribution maps, and there were also some differences in terms of detail between the two types of prediction maps due to slight differences in SBD at different locations. All maps showed a similar trend, namely high values in the central-eastern part and low ones in the northwestern and central-western parts, showing a gradual decrease from the central-eastern part to the periphery and then to the south. This is consistent with the actual land use with built-up land being concentrated in the northern and central-western regions and forest and farmland being concentrated in the central-eastern and southern parts of the country.

At the same time, different interpolation methods produced a difference in the performance of local spatial features. The spatial distribution maps predicted by IDW

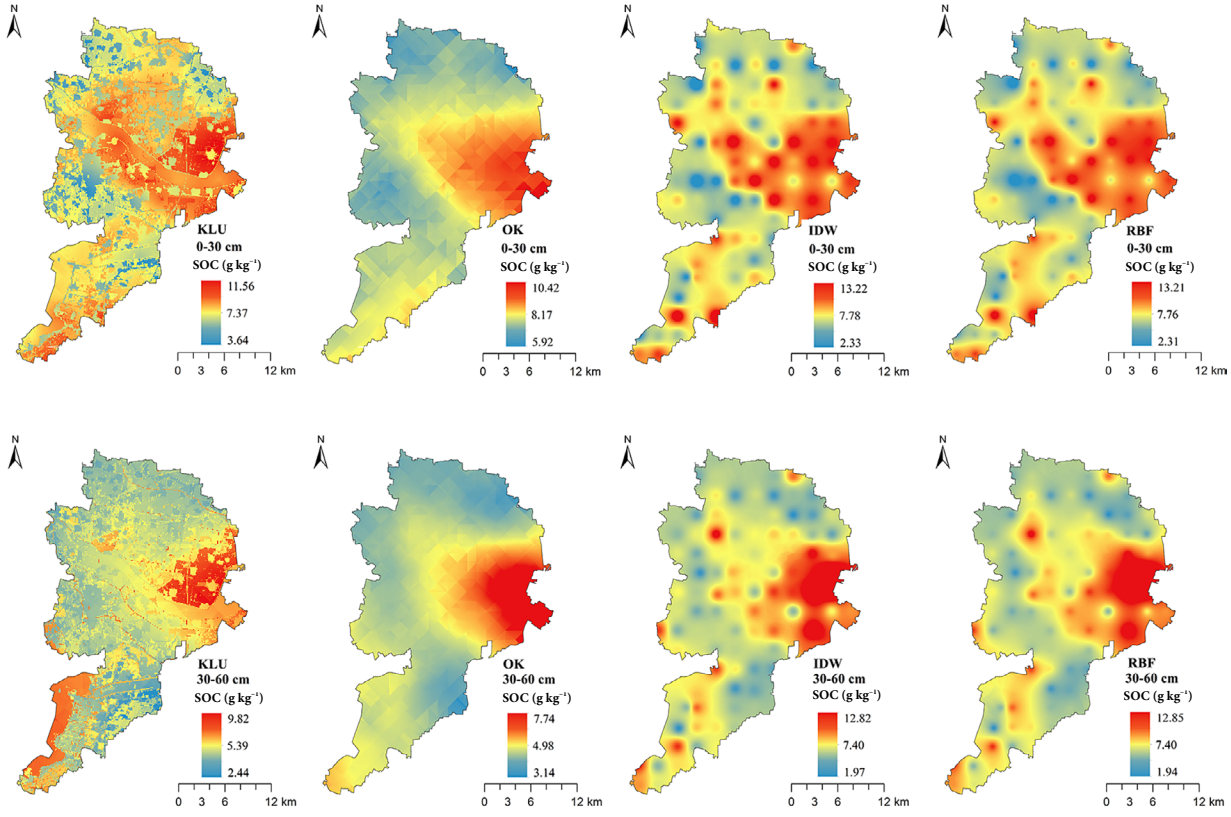

Fig. 5. Spatial distribution of SOC.

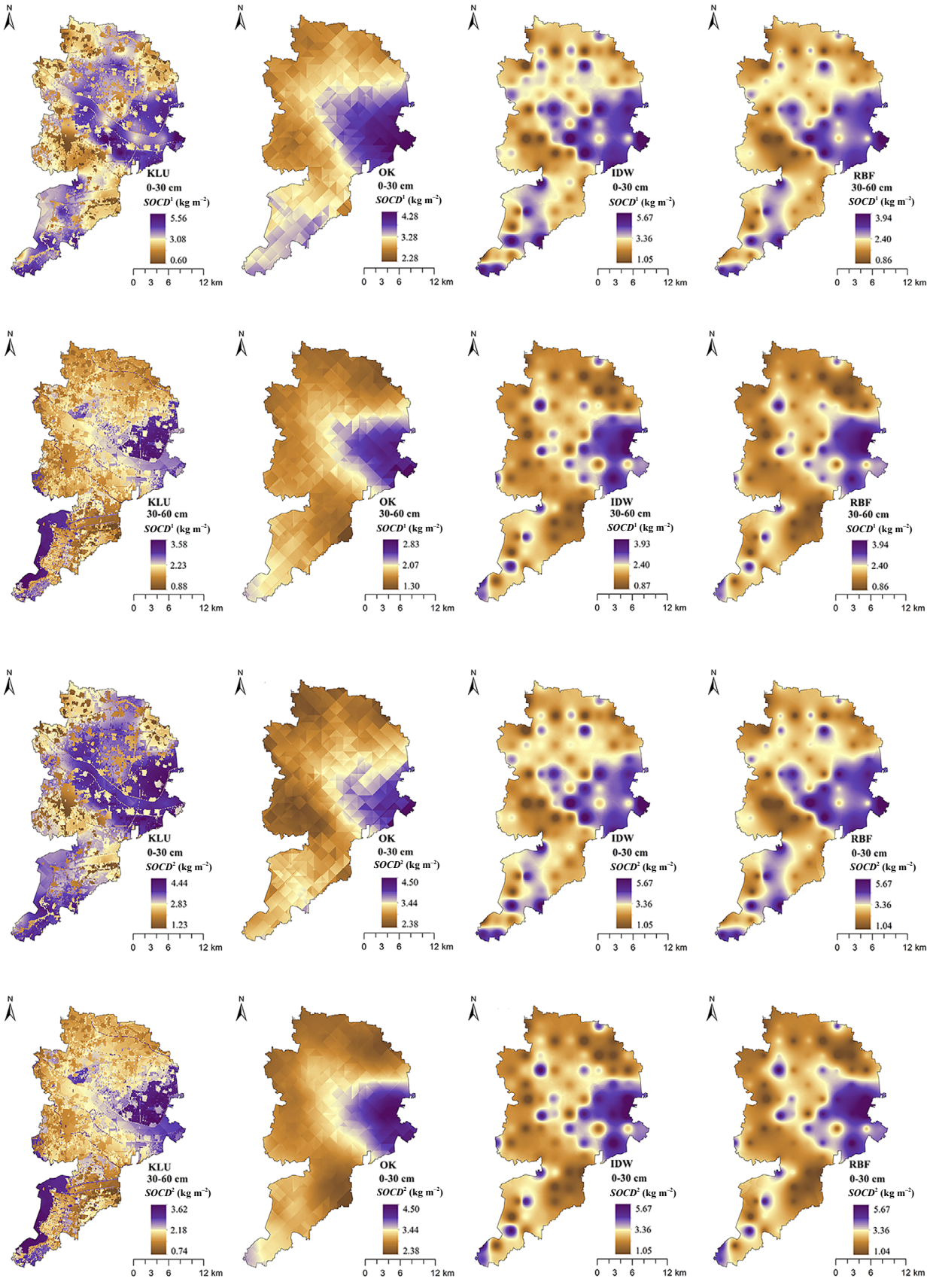

Fig. 6. Spatial distribution of $SOCD^1$ and $SOCD^2$.

Table 4. *SOCS* using different interpolation methods

Soil depth (cm)	Approaches	$SOCS^1$ (Gg)	$SOCS^2$ (Gg)
0-30	KLU	2065	2082
	OK	2087	2102
	IDW	2081	2095
	RBF	2076	2090
30-60	KLU	1385	1400
	OK	1296	1312
	IDW	1372	1384
	RBF	1371	1383

Explanation as in Table 1.

and RBF were relatively discrete, with many obvious "bull's eye" phenomena, showing local highlighting and a high degree of spatial heterogeneity; the spatial distribution maps predicted by OK vary relatively smoothly from high to low; the prediction results of the KLU method have many fragmented areas, with a high degree of similarity to the specific distribution of land use types in the study area, showing more regional distribution information.

For different soil depths, the *SOCS* results in the study area predicted using different methods did not differ significantly (Table 4). In the upper soil layer, the predicted *SOCS* values ranged from 2065 to 2103 Gg, while in the lower soil layer, the predicted *SOCS* values ranged from 1296 to 1400 Gg. The average *SOCS* value in the upper soil layer was on average 721.59 Gg higher than that in the lower soil layer, which was about 1.53 times higher than that in the lower soil layer.

DISCUSSION

The study results showed that the SOC content in the study area differed in both the vertical and horizontal distribution. In the vertical direction, the mean SOC content decreased with increasing soil depth, which is in agreement with the results that Yu *et al*. (2014) obtained in Songnen Plain and that Li *et al*. (2019) obtained in Northeast China. This is probably because the large amount of vegetation on the ground surface, the continuous accumulation of vegetation litter, long-term fertilization, tillage, and forest management practices all resulted in a much higher rate of nutrient increase in the upper soil layer than in the lower soil layer (Pan *et al*., 2010; Ghosh *et al*., 2018). At the same time, a significant degree of SOC spatial variability is found in the horizontal direction. Figure 5 shows the distribution of SOC content throughout the study area, it shows the correlation between SOC content and land use type. The SOC content varies with the land use pattern, and it is closely related to the land use type, this result is consistent with previous studies by Gelaw *et al*. (2014) and Boubehziz *et al*. (2020). From the collected soil samples (Fig. 2), the mean SOC contents of different land use types in the study area were, in descending order: built-up land < farmland < arbour forest < wetland < immature forest. Between the five land use types, the mean SOC content of the built-up land was approximately 2/3 that of the other land use types. This may be due to the fact that farmland and forest land surfaces have a large amount of vegetation which far exceeds that of built-up land, also, vegetation litterfall and root secretions are the primary sources of SOC (Bhunia *et al*., 2016) in addition, long-term fertilization, tillage, forest management and other activities were found to result in the aggregation of SOC caused by anthropogenic factors much greater than that of the influence of natural factors, thus accelerating such a phenomenon in areas other than the built-up land (Schiedung *et al*., 2019). In addition, Delelegn *et al*. (2017) found that sealing and plantation were more conducive to the increase in SOC content than farmland, which is consistent with our results that the SOC content of farmland was higher than that of built-up land but less than that of other land use types. In addition to the accumulation of dead branches, leaves and roots in the soil over time, this may be due to the fact that mature trees create a benign local microclimate that effectively prevents soil erosion. Frequent tillage, however, caused damage to the soil structure and accelerated the rate of decomposition of SOC, which in turn caused a decrease in SOC.

SOC and SBD are direct determinants of *SOCD* and *SOCS*, but accurate data concerning SBD were often lacking in previous large-scale soil inventories (Wu *et al*., 2003; Sun *et al*., 2004; Allen *et al*., 2010). For example, Wu *et al*. (2003) obtained the required SBD according to the empirical relationship between SOC content and SBD. Sun *et al*. (2004) estimated the SBD by soil type, which involved taking the average capacity weights of the same soil genus or subclass. Therefore, in order to increase the prediction accuracy of *SOCD* and *SOCS* in the study area, the SBD was recorded separately for each sampling site. It is widely believed that with changes in soil porosity and agglomerate stability, SOC and SBD will show a negative correlation trend, which in turn leads to a different spatial distribution of SOC content and *SOCD* (Whalen *et al*., 2003; Yu *et al*., 2014). However, in this study (Figs 5, 6), the spatial distributions of SOC content and *SOCD* were approximately the same throughout the study area. This result was probably due to the relatively flat terrain and homogeneity of soil types throughout the study area, which greatly contributed to the fact that SBD did not vary to a great extent across the study area.

Although *SOCS* values are influenced by various factors such as climate, vegetation, and human activities, the main determinants were found to be SOC accumulation and decomposition rates (Xue *et al*., 2015). This finding is consistent with the results of previous studies by Guan *et al*. (2015), the *SOCS* values found in this study area decreased with decreasing SOC content as the soil depth increased. The traditional method of estimating *SOCS* is to estimate the overall value using the average of soil types or land types,

which has the advantage of being a simple method but it also results in a high degree of uncertainty in the estimation of this value (Tang *et al*., 2017; Yao *et al*., 2019). In order to overcome this problem, geostatistical methods are widely used for detailed calculations. In this study, four interpolation methods were used to estimate the *SOCS* of the study area. Even though the predictions of *SOCD* varied among the different methods, the predicted total *SOCS* values were similar, which is the same conclusion that was reached by using the results of Yao *et al*. (2019). However, according to Table 3, KLU has a higher degree of accuracy as compared with other interpolation methods, so it may be considered that the total reserves predicted by KLU are closest to the actual total reserves from among the four methods.

Both structural and stochastic factors may influence the spatial distribution of soil nutrients. The more substantial the influence of structural factors such as climate, topography, and soil type, the closer the spatial correlation, while anthropogenic stochastic factors such as fertilization and tillage reduce the spatial correlation of soil nutrients (Jing *et al*., 2014; Durdevic *et al*., 2019). The variability in the effects of structural and stochastic factors on soil properties in different regions results in different degrees of spatial variability in the soil properties of different regions. No single interpolation method can always be used to obtain the most accurate result when applied to all regions and soil properties (Long *et al*., 2014). Therefore, it is important to analyse the specifics of soil properties in the study area in order to obtain a more accurate spatial distribution map.

In their study of the spatial distribution of *SOCS* and total SOC in Moscow, Russia, Vasenev *et al*. (2014) found that the spatial distribution of SOC and *SOCS* is closely related to the increase in continued urban expansion. In urban areas, rapid urban expansion and industrialization, as well as intensive human activities are the main stochastic factors responsible for the spatial variation in SOC. Among the many stochastic factors affecting the spatial variability in urban soil organic carbon, the differences between land use types are often considered to be one of the direct drivers of both high and low soil organic carbon content (Liu *et al*., 2006; James *et al*., 2019). In this study, according to Table 2, the SOC content and $SOCD^1$ in the experimental area had a weak spatial correlation, and each sampling point showed both a high degree of independence and randomness. This indicates that both stochastic and structural factors synergistically influence the spatial distribution of SOC in the Xiong'an New Area, and also, that its spatial variability is mainly regulated by stochastic factors, which is in agreement with the results of Wang *et al*. (2009) concerning urban SOC in Shenyang city. Also, differences in land use were found to significantly affect soil nutrients (Fig. 2), with soil nutrient contents usually being similar for the same land use type and significantly different for different land use types. In calculating the semivariance function, the original data was compared with the residuals, the $C_0/(C_0+C)$ values of both were reduced by different degrees after removing the mean values of SOC content and *SOCD* under different land use types, the effects of stochastic factors were effectively reduced, thereby indicating that it is feasible to use land use types as auxiliary variables for spatial prediction in this study.

The prediction results produced by different interpolation methods were compared, and significant differences were found between the different prediction methods (Table 3). The interpolation results of KLU were found to be more accurate compared with those of the other three interpolation methods, and its predicted spatial distribution map was found to be more representative of the actual regional spatial pattern. In addition, as shown in Figs 5 and 6, the different land use types in the study area have obvious effects on the spatial distribution of SOC content and density, and also show significant differences in the spatial distribution maps. The prediction produced using the OK method mainly reflects the overall situation of the study area, which focuses on the interconnection between the sample point locations, and although the outliers are effectively avoided, the minimum values of the soil properties are overestimated and the maximum values are underestimated due to the smoothing effect, this results in a lack of local detail information (Pang *et al*., 2011; Tripathi *et al*., 2015). Although the extreme values are considered in IDW and RBF, IDW and RBF are both susceptible to the influence of measured data and emphasize local volatility (Xu *et al*., 2015). By contrast, the prediction results produced by the KLU method not only reflect the interconnection between the sample point locations, but also show the variability in the actual spatial distribution of SOC in the study area due to land use. In agreement with the results produced by this study, Long *et al*. (2020) in southeast China and Boubehziz *et al*. (2020) in northeast Algeria also found that using auxiliary variables can effectively improve the interpolation accuracy and reduce the influence of external factors on soil variables.

As shown in Table 3, the KLU prediction accuracy of $SOCD^2$ is highest in the upper soil layer, while the KLU prediction accuracy of $SOCD^1$ was found to be more accurate in the lower soil layer. This phenomenon may be due to the fact that the upper layer of soil is close to the surface. The SOC content and SBD of the upper layer are more independent and random as compared to the situation in the lower layer of soil (Table 2), these values are more substantially influenced by land use. The KLU of Method 2 considers the influence of land use on SOC content and SBD at the same time, while Method 1 considers the influence of land use only once, therefore the degree of error produced by Method 1 was greater than of Method 2. The lower layer of soil is less profoundly affected by human activities, while the error in spatial analysis in terms of the SOC content and SBD exceeds the error of direct spatial analysis of *SOCD*, therefore Method 1 has a greater degree of prediction accuracy.

Although KLU was found to significantly improve the prediction accuracy of SOC distribution in the study area, the predicted values still differed from the measured ones (Table 3). In addition to land use type, other natural factors such as topography, terrain, and climate may also synergistically affect the spatial distribution of SOC. For example, Zhang *et al*. (2018) demonstrated that topographic elements were essential drivers of SOC content in the grassland soils of the hilly areas of northern China. Zhang *et al*. (2019) concluded that topography and land use practices influenced SOC distribution in a hilly region of the Loess Plateau, and also, that there was a significant degree of interaction between them. Brovelli *et al*. (2012) found that SOC in riparian soils fluctuated with climate change. In addition, the selection of samples in the study area also affects the interpolation accuracy. Zhang *et al*. (2021) compared the interpolation accuracy of *SOCS* in the Karst Region at different sampling distances, and it was concluded that the interpolation accuracy varied with sample distance. When interpolating in flat areas, it is more sensitive to the distribution of sample points than when interpolating in complex terrain (Long *et al*., 2018). In summary, in order to further improve the accuracy of the spatial distribution of SOC content and density in the study area, the next step should be to consider the natural factors and the actual influence of sample point distribution.

CONCLUSIONS

1. As an urban area with frequent human activities and diverse land use patterns, the Xiong'an New Area has a large degree of spatial variability in terms of soil organic carbon. The soil organic carbon content decreased with increasing soil depth and was significantly affected by different land use types ($p<0.05$).

2. In this paper, the spatial distributions of soil organic carbon content and density in the 0-30 cm and 30-60 cm soil layers were studied by applying four interpolation methods, kriging combined with land use, ordinary kriging, inverse distance weighting and radial basis function, using measured data from 91 sampling points, and the soil organic carbon stocks was estimated. The results showed that land use significantly influenced the spatial distribution of soil organic carbon in the Xiong'an New Area. Traditional interpolation methods (*i.e.*, ordinary kriging, inverse distance weighting, radial basis function) produced a low degree of interpolation accuracy for soil organic carbon content and density, while kriging combined with land use, which incorporates auxiliary variables, effectively eliminated the differences in soil organic carbon content and density distributions caused by different land use types, and provided more accurate soil organic carbon stocks prediction results.

3. Land use type obviously influences the spatial distribution of soil organic carbon in urban areas, and by using land use type as auxiliary data, a more accurate spatial distribution of soil organic carbon and prediction of its total storage capacity may be estimated. By using the Xiong'an New Area as a research object, it is intended to provide the basis for urban planning and development and also urban land management based on this research.

ACKNOWLEDGMENTS

The authors are grateful to the Fundamental Research Funds of CAF (CAFYBB2019ZB005).

Conflicts of Interest: The authors declare that they have no known competing financial interests or personal relationships that could have appeared to influence the work reported in this paper.

REFERENCES

Allen D.E., Pringle M.J., Page K.L., and Dalal R.C., 2010. A review of sampling designs for the measurement of soil organic carbon in Australian grazing lands. Rangel. J., 32, 227-246, https://doi.org/10.1071/RJ09043

Bao S.D., 2005. Soil agrochemical analysis. China Agriculture Press, Beijing, China.

Barreto M.S.C., Schellekens J., Ramlogan M., Rouff A.A., Elzinga E.J., Vidal-Torrado P., and Alleoni L.R.F., 2021. Effects of horticulture on soil organic matter properties in highly weathered tropical soils. Soil Tillage Res., 213, 105156, https://doi.org/10.1016/j.still.2021.105156

Bhunia G.S., Shit P.K., and Maiti R., 2016. Comparison of GIS-based interpolation methods for spatial distribution of soil organic carbon (SOC). J. Saudi Soc. Agric. Sci., 17, 114-126, https://doi.org/10.1016/j.jssas.2016.02.001

Blais E., 2021. Carbon sequestration and the urban heat island effect. VCU Environmental Research Methods, QUBES Educational Resources, https://doi.org/10.25334/ZRXW-ZB81

Blanchet G., Libohova Z., Joost S., Rossier N., Schneider A., Jeangros B., and Sinaj S., 2017. Spatial variability of potassium in agricultural soils of the canton of Fribourg, Switzerland. Geoderma, 290, 107-121, https://doi.org/10.1016/j.geoderma.2016.12.002

Boubehziz S., Khanchoul K., Benslama M., Benslama A., Marchetti A., Francaviglia R., and Piccini C., 2020. Predictive mapping of soil organic carbon in Northeast Algeria. Catena, 190, 104539, https://doi.org/10.1016/j.catena.2020.104539

Brovelli A., Batlle-Aguilar J., and Barry D.A., 2012. Analysis of carbon and nitrogen dynamics in riparian soils: Model development. Sci. Total Environ., 429, 231-245, https://doi.org/10.1016/j.scitotenv.2012.04.027

Cambardella C.A., Moorman T.B., Novak J.M., Parkin T.B., Karlen D.L., Turco R.F., and Konopka A.E., 1994. Field-scale variability of soil properties in central Iowa soils. Soil Sci. Soc. Am. J., 58, 1501-1511, https://doi.org/10.2136/sssaj1994.03615995005800050033x

Davidson E.A. and Janssens I.A., 2006. Temperature sensitivity of soil carbon decomposition and feedbacks to climate change. Nature, 440, 165-173, https://doi.org/10.1038/nature04514

Delelegn Y.T., Purahong W., Blazevic A., Yitaferu B., Wubet T., Goransson H., and Godbold D.L., 2017. Changes in land use alter soil quality and aggregate stability in the highlands of northern Ethiopia. Sci. Rep., 7, 13602, https://doi.org/10.1038/s41598-017-14128-y

Deng X., Chen X., Ma W., Ren Z., Zhang M., Grieneisen M.L., Long W., Ni Z., Zhan Y., and Lv X., 2018. Baseline map of organic carbon stock in farmland topsoil in East China. Agric. Ecosyst. Environ., 254, 213-223, https://doi.org/10.1016/j.agee.2017.11.022

Durdevic B., Jug I., Jug D., Bogunovic I., Vukadinovic V., Stipesevic B., and Brozovic B., 2019. Spatial variability of soil organic matter content in Eastern Croatia assessed using different interpolation methods. Int. Agrophys., 33(1), 31-39, https://doi.org/10.31545/intagr/104372

Gelaw A.M., Singh B.R., and Lal R., 2014. Soil organic carbon and total nitrogen stocks under different land uses in a semi-arid watershed in Tigray, Northern Ethiopia. Agric. Ecosyst. Environ., 188, 256-263, https://doi.org/10.1016/j.agee.2014.02.035

Ghosh A., Bhattacharyya R., Meena M.C., Dwivedi B.S., Singh G., Agnihotri R., and Sharma C., 2018. Long-term fertilization effects on soil organic carbon sequestration in an Inceptisol. Soil Tillage Res., 177, 134-144, https://doi.org/10.1016/j.still.2017.12.006

Guan F., Tang X., Fan S., Zhao J., and Peng C., 2015. Changes in soil carbon and nitrogen stocks followed the conversion from secondary forest to Chinese fir and Moso bamboo plantations. Catena, 133, 455-460, https://doi.org/10.1016/j.catena.2015.03.002

Hebei Statistical Bureau, 2021. Hebei Statistical Yearbook (in Chinese). China Statistics Press, Beijing.

Hopple A.M., Wilson R.M., Kolton M., Zalman C.A., Chanton J.P., Kostka J., Hanson P.J., Keller J.K., and Bridgham S.D., 2020. Massive peatland carbon banks vulnerable to rising temperatures. Nat. Commun., 11, 1-7, https://doi.org/10.1038/s41467-020-16311-8

James J.N., Gross C.D., Dwivedi P., Myers T., Santos F., Bernardi R., Faria M.F.D., Guerrini I.A., Harrison R., and Butman D., 2019. Land use change alters the radiocarbon age and composition of soil and water-soluble organic matter in the Brazilian Cerrado. Geoderma, 345, 38-50, https://doi.org/10.1016/j.geoderma.2019.03.019

Janzen H.H., 2004. Carbon cycling in earth systems – a soil science perspective. Agric Ecosyst. Environ., 104, 399-417, https://doi.org/10.1016/j.agee.2004.01.040

Jing L., Qingwen M., Wenhua L., Yanying B., and Zheng Y., 2014. Spatial variability analysis of soil nutrients based on GIS and geostatistics: a case study of Yisa township, Yunnan, China. J. Res. Ecol., 5, 348-355, https://doi.org/10.5814/j.issn.1674-764x.2014.04.010

Johnston C.A., Groffman P., Breshears D.D., Cardon Z.G., Currie W., Emanuel W., Gaudinski J., Jackson R.B., Lajtha K., Nadelhoffer K., Nelson D.Jr., Post W.M., Retallack G., and Wielopolski L., 2004. Carbon cycling in soil. Front. Ecol. Environ., 2, 522-528, https://doi.org/10.1890/1540-9295(2004)002[0522:CCIS]2.0.CO;2

Joss S., Cowley R., and Tomozeiu D., 2013. Towards the 'ubiquitous eco-city': an analysis of the internationalisation of eco-city policy and practice. Urban Research & Practice, 6, 54-74, https://doi.org/10.1080/17535069.2012.762216

Keith H., Vardon M., Obst C., Young V., Houghton R.A., and Mackey B., 2021. Evaluating nature-based solutions for climate mitigation and conservation requires comprehensive carbon accounting. Sci. Total Environ., 769, 144341, https://doi.org/10.1016/j.scitotenv.2020.144341

Kirschbaum M.U.F., 2000. Will changes in soil organic carbon act as a positive or negative feedback on global warming? Biogeochemistry, 48, 21-51, https://doi.org/10.1023/A:1006238902976

Lal R., 2004. Soil carbon sequestration impacts on global climate change and food security. Science, 304, 1623-1627, https://doi.org/10.1126/science.1097396

Li M., Han X., Du S., and Li L.J., 2019. Profile stock of soil organic carbon and distribution in croplands of Northeast China. Catena, 174, 285-292, https://doi.org/10.1016/j.catena.2018.11.027

Liu T.L., Juang K.W., and Lee D.Y., 2006. Interpolating soil properties using kriging combined with categorical information of soil maps. Soil Sci. Soc. Am. J., 70, 1200-1209, https://doi.org/10.2136/sssaj2005.0126

Liu Y., He N., Zhu J., Xu L., Yu G., Niu S., Sun X., and Wen X., 2017. Regional variation in the temperature sensitivity of soil organic matter decomposition in China's forests and grasslands. Glob. Chang. Biol., 23, 3393-3402, https://doi.org/10.1111/gcb.13613

Long J., Liu Y., Xing S., Zhang L., Qu M., Qiu L., Huang Q., Zhou B., and Shen J., 2020. Optimal interpolation methods for farmland soil organic matter in various landforms of a complex topography. Ecol. Indic., 110, 105926, https://doi.org/10.1016/j.ecolind.2019.105926

Long J., Liu Y.L., Xing S.H., Qiu L.X., Huang Q., Zhou B.Q., Shen J.Q., and Zhang L.M., 2018. Effects of sampling density on interpolation accuracy for farmland soil organic matter concentration in a large region of complex topography. Ecol. Indic., 93, 562-571, https://doi.org/10.1016/j.ecolind.2018.05.044

Long J., Zhang L.M., Shen J.Q., Zhou B.Q., Mao Y.L., Qiu L.X., and Xing S.H., 2014. Spatial interpolation of soil organic matter in farmlands in areas complex in landform (in Chinese). Acta Petrol. Sin., 51, 1270-1281.

Luo Z., Luo Y., Wang G., Xia J., and Peng C., 2020. Warming-induced global soil carbon loss attenuated by downward carbon movement. Glob. Chang. Biol., 26, 7242-7254, https://doi.org/10.1111/gcb.15370

Mabit L. and Bernard C., 2010. Spatial distribution and content of soil organic matter in an agricultural field in eastern Canada, as estimated from geostatistical tools. Earth Surf. Process. Landf., 35, 278-283, https://doi.org/10.1002/esp.1907

Minasny B., Malone B.P., McBratney A.B., Angers D.A., Arrouays D., Chambers A., Chaplot V., Chen Z.-S., Cheng K., Das B.S., Field D.J., Gimona A., Hedley C.B., Hong S.Y., Mandal B., Marchant B.P., Martin M., McConkey B.G., Mulder V.L., O'Rourke S., Richer-de-Forges A.C., Odeh I., Padarian J., Paustian K., Pan G., Poggio L., Savin I., Stolbovoy V., Stockmann U., Sulaeman Y., Tsui C.-C., Vågen T.-G., van Wesemael B., and Winowiecki L., 2017. Soil carbon 4 per mille. Geoderma, 292, 59-86, https://doi.org/10.1016/j.geoderma.2017.01.002

Ministry of Natural Resources, People's Republic of China, 2017. Current Land Use Classification: GB/T 2010-2017. China Zhijian Publishing House, Beijing, China.

Pan G., Xu X., Smith P., Pan W., and Lal R., 2010. An increase in topsoil SOC stock of China's croplands between 1985 and 2006 revealed by soil monitoring. Agric. Ecosyst. Environ., 136, 133-138, https://doi.org/10.1016/j.agee.2009.12.011

Pang S., Li T.X., Zhang X.F., Wang Y.D., and Yu H.Y., 2011. Spatial variability of cropland lead and its influencing factors: A case study in Shuangliu county, Sichuan province, China. Geoderma, 162, 223-230, https://doi.org/10.1016/j.geoderma.2011.01.002

Panja P., 2021. Deforestation, Carbon dioxide increase in the atmosphere and global warming: A modelling study. Int. J. Simul. Model., 41, 209-219, https://doi.org/10.1080/02286203.2019.1707501

Robinson T.P. and Metternicht G.M., 2006. Testing the performance of spatial interpolation techniques for mapping soil properties. Comput. Electron. Agric., 50, 97-108, https://doi.org/10.1016/j.compag.2005.07.003

Scharlemann J.P.W., Tanner E.V.J., Hiederer R., and Kapos V., 2014. Global soil carbon: understanding and managing the largest terrestrial carbon pool. Carbon Manag., 5, 81-91, https://doi.org/10.4155/cmt.13.77

Schiedung M., Tregurtha C.S., Beare M.H., Thomas S.M., and Don A., 2019. Deep soil flipping increases carbon stocks of New Zealand grasslands. Glob. Chang. Biol., 25, 2296-2309, https://doi.org/10.1111/gcb.14588

Stockmann U., Adams M.A., Crawford J.W., Field D.J., Henakaarchchi N., Jenkins M., Minasny B., McBratney A.B., Courcelles de V.R., Singh K., Wheeler I., Abbott L., Angers D.A., Baldock J., Bird M., Brookes P.C., Chenu C., Jastrow J.D., Lal R., Lehmann J., O'Donnell A.G., Parton W.J., Whitehead D., and Zimmermann M., 2013. The knowns, known unknowns and unknowns of sequestration of soil organic carbon. Agric. Ecosyst. Environ., 164, 80-99, https://doi.org/10.1016/j.agee.2012.10.001

Sun W.X., Shi X.Z., Yu D.S., Wang K., and Wang H.J., 2004. Estimation of soil organic carbon storage based on 1 : 1 M soil database of China (in Chinese). Sci. Geol. Sin., 24, 568-572.

Tang X., Xia M., Pérez-Cruzado C., Guan F., and Fan S., 2017. Spatial distribution of soil organic carbon stock in Moso bamboo forests in subtropical China. Sci. Rep., 7, 1-13, https://doi.org/10.1038/srep42640

Tripathi R., Nayak A.K., Shahid M., Raja R., Panda B.B., Mohanty S., Kumar A., Lal B., Gautam P., and Sahoo R.N., 2015. Characterizing spatial variability of soil properties in salt affected coastal India using geostatistics and kriging. Arab. J. Geosci., 8, 10693-10703, https://doi.org/10.1007/s12517-015-2003-4

Vasenev V.I., Stoorvogel J.J., Vasenev I.I., and Valentini R., 2014. How to map soil organic carbon stocks in highly urbanized regions? Geoderma, 226, 103-115, https://doi.org/10.1016/j.geoderma.2014.03.007

Viscarra Rossel R.A., Webster R., Bui E.N., and Baldock J.A., 2014. Baseline map of organic carbon in Australian soil to support national carbon accounting and monitoring under climate change. Glob. Chang. Biol., 20, 2953-2970, https://doi.org/10.1111/gcb.12569

Wang Q.B., Duan Y.Q., and Wei Z.Y., 2009. Spatial variability of urban soil organic carbon in Shenyang City (in Chinese). Chin. J. Soil Sci., 40, 252-257.

Whalen J.K., Willms W.D., and Dormaar J.F., 2003. Soil carbon, nitrogen and phosphorus in modified rangeland communities. Rangel. Ecol. Manag., 56, 665-672, https://doi.org/10.2307/4003944

Wu H., Guo Z., and Peng C., 2003. Land use induced changes of organic carbon storage in soils of China. Glob. Chang. Biol., 9, 305-315, https://doi.org/10.1046/j.1365-2486.2003.00590.x

Xu D., Liu C.H., Cai T.Y., and Zhang S.E., 2015. 3D spatial distribution characteristics of soil organic matter and total nitrogen in farmland (in Chinese). Transactions of the Chin. Soc. Agric. Machin., 46, 157-163.

Xu Y., Sun X., and Tang Q., 2016. Human activity intensity of land surface: Concept, method and application in China. J. Geogr. Sci., 26, 1349-1361, https://doi.org/10.1007/s11442-016-1331-y

Xue Z., Ma L., An S., and Wang W., 2015. Soil organic carbon density and stock at the catchment scale of a hilly region of the loess plateau (in Chinese). Acta Ecological Sinica, 35, 2917-2925, https://doi.org/10.5846/stxb201311262813

Yan Y., Zhang C., Hu Y., and Kuang W., 2015. Urban land-cover change and its impact on the ecosystem carbon storage in a dryland city. Remote Sens., 8, 6, https://doi.org/10.3390/rs8010006

Yang Y., Mohammat A., Feng J., Zhou R., and Fang J., 2007. Storage, patterns and environmental controls of soil organic carbon in China. Biogeochemistry, 84, 131-141, https://doi.org/10.1007/s10533-007-9109-z

Yao R., Yang J., Liu G., and Zou P., 2006. Spatial variability of soil salinity in characteristic field of the Yellow River Delta (in Chinese). Transactions of the CSAE, 22, 61-66.

Yao X., Yu K., Deng Y., Zeng Q., Lai Z., and Liu J., 2019. Spatial distribution of soil organic carbon stocks in Masson pine (*Pinus massoniana*) forests in subtropical China. Catena, 178, 189-198, https://doi.org/10.1016/j.catena.2019.03.004

Ye J., Hu Y., Zhen L., Wang H., and Zhang Y., 2021. Analysis on land use Change and its driving mechanism in Xilingol, China, during 2000-2020 using the Google Earth engine. Remote Sens., 13, 5134, https://doi.org/10.3390/rs13245134

Yu P.J., Li Q., Jia H.T., Li G.D., Zheng W., Shen X.J., Diabate B., and Zhou D.W., 2014. Effect of cultivation on dynamics of organic and inorganic carbon stocks in Songnen plain. Agron. J., 106, 1574-1582, https://doi.org/10.2134/agronj14.0113

Zhang X.Y., Liu M.Z., Zhao X., Li Y.Q., Zhao W., Li A., Chen S., Chen S.P., Han X.G., and Huang J.H., 2018. Topography and grazing effects on storage of soil organic carbon and nitrogen in the northern China grasslands. Ecol. Indic., 93, 45-53, https://doi.org/10.1016/j.ecolind.2018.04.068

Zhang Y., Li P., Lie X., Zhao B., and Peng S., 2019. Effects of topography and land use on soil organic carbon in hilly region of Loess Plateau (in Chinese). Acta Pedo. Sin., 56, 1140-1149.

Zhang Z., Zhou Y., and Huang X., 2021. Exploring the optimal sampling density to characterize spatial heterogeneity of soil carbon stocks in a Karst Region. Agron. J., 113, 99-110, https://doi.org/10.1002/agj2.20467

Zou Y. and Zhao W., 2018. Making a new area in Xiong'an: Incentives and challenges of China's "Millennium Plan". Geoforum, 88, 45-48, https://doi.org/10.1016/j.geoforum.2017.11.00